Journal of
Ceramic Science
and Technology

J. Ceram. Sci. Tech., **08** [01] 39-44 (2017)
DOI: 10.4416/JCST2016-00071
available online at: http://www.ceramic-science.com

Effect of Laser Power on Yield of TiO_2 Nanoparticles Synthesized by Pulsed Laser Ablation in Water

A. Singh*[1], J. Vihinen[2], E. Frankberg[1], L. Hyvärinen[1], M. Honkanen[1], E. Levänen[1]

[1]Department of Materials Science, Tampere University of Technology, P. O. Box 589, FIN 33101 Tampere, Finland
[2]Department of Mechanical Engineering and Industrial Systems, Tampere University of Technology, P. O. Box 589, FIN 33101 Tampere, Finland
received September 19, 2016; received in revised form November 15, 2016; accepted December 9, 2016

Abstract

In this study, the pulsed laser ablation in liquids (PLAL) technique was used on titanium in deionized water at different laser powers to understand its effect on the synthesis yield of nanoparticles. A 500-ns 1062-nm fiber laser at 25 kHz was used to effect PLAL of titanium to produce nanoparticles. TEM images of the synthesized nanoparticles showed spherical particles ranging from 3 – 32 nm in diameter. The electron diffraction pattern and high peaks in the wide-angle x-ray scattering (WAXS) pattern indicated high crystallinity of nanoparticles. WAXS results showed nanoparticles were allotropes of titania: rutile and anatase. Synthesis yield measurements indicated an increase in yield with the increase in laser power as long as the increase in laser fluence remains proportional to the increase in laser power. However, the yield increased proportionally with the increase in laser fluence. The analysis of the chosen laser pulse duration and repetition rate showed an increase in the yield with longer pulse duration and higher repetition rate.

Keywords: Nanoparticles, synthesis yield, pulsed laser ablation in liquids, WAXS, laser fluence

I. Introduction

Synthesis and use of nanoparticles accounts for a large part of the burgeoning nanoparticle industry in the world. Photoactive TiO_2 nanoparticles have several applications such as water purification, self-cleaning, anti-bacterial, and anti-fogging [1,2]. The use of pulsed laser ablation in liquids (PLAL) has been well reported by many researchers for the synthesis of nanoparticles of metals and metal oxides [3–6]. PLAL has been reported as a green method for the production of nanomaterials with reproducible results and it costs about € 20k for the experimental equipment including the laser [7]. In PLAL, a pulsed laser irradiates a target that is dipped in a solvent to produce nanoparticles. The optical breakdown of the water by the pulsed laser leads to the formation of cavitation bubbles, inside which the generation and growth of nanoparticles occur [8,9]. Upon the collapse of the cavitation bubble, these nanoparticles are released into the surrounding liquid to form a nanoparticle suspension [9]. The synthesis parameters are classified into two groups: laser parameters (such as laser power, fluence, duration, wavelength and repetition rate) and material parameters (such as target material, solvent, temperature and pressure of the system) [10].

Due to the lack of universally defined procedures for PLAL[10], and availability of numerous laser and material parameters, there are no conclusive results on the effect of laser parameters, such as laser power and laser fluence, on the synthesis yield of TiO_2 nanoparticles. This study aims to fill this research gap by experimental investigation of the variation in synthesis yield of nanoparticles. In this study, we determined how the laser parameters – laser power and laser fluence – affect the synthesis yield of TiO_2 nanoparticles.

II. Materials and Methods

A suspension of nanoparticles was obtained via irradiation of titanium metal plate (99.99 % pure, Goodfellow Cambridge Ltd) by 85W 500-nanosecond fiber laser at 1062 nm output using a XY scanner. The laser was an SPI 85 Watt fiber laser obtained from SPI Lasers Limited with the model name SPI SP-085-W-HS-M-B-Y(02). The beam quality factor or beam propagation factor M^2 was 3.7. The laser was controlled by SPI's software G4 Laser control (version 4.0). The scanner was a GSI HB X-10 with an aperture of 10 mm and consisted of two mirrors. The optics consisted of a Linos f-theta Ronar objective lens with 160 mm focal length obtained from LINOS photonics. The scanner was controlled by SCAPS software SAM-Light (version 3.0.5) from SCAPS GmbH. The laser beam was focused on the titanium target by the f-theta lens on a predetermined area 8 mm x 8 mm on the titanium target. The pulse duration was 500 ns and repetition rate was 25 kHz. The maximum pulse energy of the laser was 3.4 mJ

* Corresponding author: amandeep.singh@tut.fi

per pulse and was available at 500-nanosecond pulse duration, which is the time for which the laser pulse irradiates the target. The maximum laser fluence of the laser was 58.92 J/cm^2. The scanning speed was 2000 mm/s for each experiment. The collimated laser beam diameter was 8.5 mm provided by the manufacturer of the laser SPI Lasers Ltd. At this speed, the scanner took 2.566 seconds to complete one loop on an area of 8 mm x 8 mm. Each experiment consisted of 720 loops, which corresponds to an ablation time of 30 minutes. During irradiation of the titanium target, the plasma plume formed as a result of ablation, was clearly visible with the naked eye. A visible blue coloration of DIW was observed after about 20 loops due to laser ablation of titanium resulting in the removal of material from target to the surrounding liquid DIW.

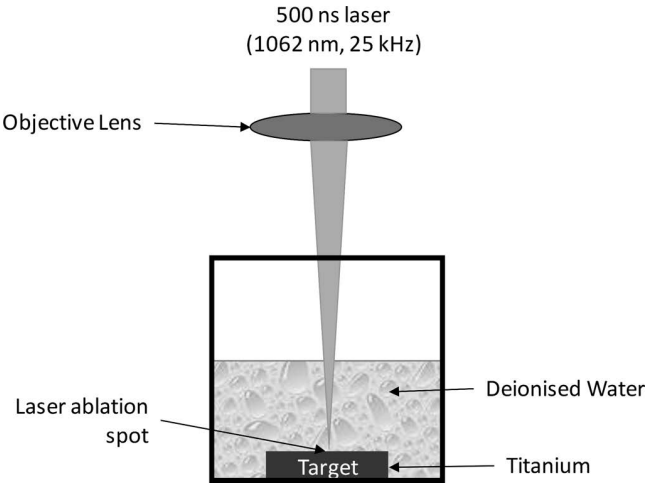

Fig. 1: Schematic of pulsed laser ablation of titanium in deionized water.

PLAL of titanium plate was performed in deionized water (DIW) with laser powers 12 %, 15 %, 18 %, 20 %, 30 %, 40 %, and 50 % of the maximum laser power. The titanium targets, 15 mm x 15 mm, were completely identical for ablation experiments at each chosen laser power. The thickness of DIW film above titanium target was 5 mm. As the ablation was performed in water, the focusing of the laser depended not only on the target position relative to the focusing lens but also on the thickness of the water film on top of target. Due to higher refractive index of water (1.33) compared to air (1.00), the 5-mm-thick layer of DIW above the target shifts the focal plane as a result of optical refraction in water. So, the laser must be focused on the target only after adjusting the water film thickness, which in this case was 5 mm. In all the experiments, the target-objective lens distance and thickness of water film was the same in order to have identical focusing conditions. The ablation time was also the same, 30 minutes, in each case to synthesize nanoparticle suspensions. The laser beam was incident at an angle of 90° relative to the target surface plane to effect ablation (as shown in Fig. 1). The vessel containing the titanium target dipped in DIW was placed on a horizontal platform and the irradiation was performed from the top at an angle of 90° as mentioned earlier. All laser and scanning parameters were exactly same for all samples and the only variable parameter was the laser power which was used for controlling the laser fluence. The pulse energy and laser output varied linearly with each other. The correlation was determined experimentally using a FieldMaxII-TOP energy meter and PM300F-50 sensor from Coherent Inc. (USA). Therefore, the term laser power is synonymous with pulse energy, and so this manuscript can also be interpreted as the "Effect of the laser pulse energy on the yield of TiO_2 nanoparticles synthesized by pulsed laser ablation." The spot diameters were measured for different laser powers by ablating the target in air medium at normal atmosphere pressure and room temperature and measuring the diameter of the ablated crater from the optical microscopy images. The parameters used for the laser and scanner were 500 ns pulse duration, 25 kHz repetition rate, 2000 mm/s scanning speed. As mentioned earlier, the beam quality factor M^2 was 3.7, which for an ideal laser should be 1. Due to this, the spot diameter varied with the variation in laser power.

The samples for measuring the synthesis yield were prepared from these synthesized suspensions. Small LDPE bottles, ordered from VWR International Limited, were used for storing the synthesized nanoparticle suspensions. 10 ml of each suspension type was then pipetted to the respective vial and dried in a heat cabin at a constant temperature of 120 °C to obtain the nanoparticle powder. These dried powders were then weighed to measure the yield of nanoparticles for varying laser powers. Since the ablation time in each case was 30 minutes, the mass of nanoparticles produced is proportional to the productivity of nanoparticles for each value of laser power.

The obtained suspensions were characterized by means of transmission electron microscopy (TEM) and wide-angle x-ray scattering (WAXS). TEM images of the nanoparticles were taken using a Jeol JEM-2010 microscope. Imaging in each case was performed at 200 kV acceleration voltage. TEM samples were prepared from droplets of the synthesized suspensions dried out on carbon-coated copper grids. A Panalytical Empyrean Multipurpose Diffractometer with anode material copper using CuKα radiation (λ = 0.15418 nm) was used for WAXS measurements. It was powered by an x-ray generator at 45 kV and 40 mA. It consisted of a solid-state pixel detector, PIXcel3D, which measured the scattered intensities as a function of the scattering angle (2θ). To prepare the WAXS sample, an equal volume of each suspension was enclosed between two Mylar foils which were x-ray transparent. They were then placed between the respective circular transmission holders for each sample. The background sample was DIW enclosed between two Mylar foils. The phase identification from WAXS pattern was done with Panalytical HighScore Plus software (version 3.0.5). The scan range was from 5.0° to 54.9° with a 0.026° step size.

III. Results and Discussion

This study used a 1062-nm fiber laser, which is a near-infrared region (NIR) laser. This raises question about the interaction of the 1062-nm fiber laser with water, or precisely how significant is the absorption of the laser light by DIW. Altınoğlu *et al.* reported that the absorption coefficient of water is minimal from a wavelength of 800 nm

and till 1150 nm in NIR [11]. Due to insignificant absorption, wavelengths between 800 nm and 1000 nm constitute to form the highest optical transmission window, also known as "imaging window" for the laser light in water. The absorption coefficient of water at 1062 nm also lies in this highest optical transmission window in NIR. 1319, 1320 nm, and 1470 nm are some of the specific wavelengths for high absorption coefficient of light by water in NIR [12]. Due to this, in our study, there was insignificant absorption of laser light by water. However, the quenching of target, and especially target surface undergoing ablation, resulted in heating of water. The ablation of titanium target in DIW was observed to begin at a laser fluence of 13.85 J/cm^2. In literature, the ablation threshold of titanium with a 4.5-ns Nd:YAG laser at 10 kHz was reported to be 4.5 J/cm^2 in air [13]. This implies a threefold increase in the threshold in DIW compared to air. In literature, similar results were reported by Kabashin *et al.*, in which the ablation threshold of gold was found to be five times higher in water compared to vacuum [14]. The ablation was caused by the pulsed laser at 25 kHz repetition rate which means that the time interval between two laser pulses was 40 µs. This is several times shorter than the duration of cavitation bubble ~ 600 µs. This suggests that the subsequent laser pulses pass through the cavitation bubble, which acts as a negative lens and leads to defocusing of the laser. In our previous study, we have discussed the photothermal mechanism for nanoparticle formation by pulsed laser ablation in DIW with the same laser and laser parameters as in this study [6]. With a nanosecond laser, the nanoparticles are formed by photothermal mechanisms, such as vaporization and boiling [15]. So, with this 500-ns laser, we can exclude "Coulomb explosion" as a nanoparticles formation mechanism.

Fig. 2 shows TEM images of nanoparticles synthesized by laser ablation of titanium. The nanoparticles were spherical in shape and formed a web-like network in which all particles are joined to form a cluster of nanoparticles (Fig. 2b). There are then several individual clusters in the nanoparticles suspensions. The size range of nanoparticles measured from TEM images in Fig. 2 (a) was 3 – 32 nm with a mean diameter of 8.1 nm. When the nuclei-containing clusters of ablated metal atoms join to form nanoparticles inside the cavitation bubbles, the temperature is high enough to cause melting of these nuclei to form spherical nanoparticles [10]. The spherical shape results in minimizing the interfacial energy.

ED pattern analysis and high peaks in the WAXS pattern (Fig. 3) indicated that the nanoparticles synthesized were crystalline. WAXS analysis of nanoparticle suspension synthesized at 20 % laser power showed that the nanoparticles were titania (TiO_2) allotropes; rutile and anatase. The highest-intensity peaks detected for rutile and anatase were at scattering angles (2θ) 27.4° and 25.3° respectively. The formation of an oxide of titanium was anticipated since the solvent, DIW, is a source of oxygen. There were no peaks in the pattern for any other titanium compounds or titanium metal. Absence of peaks for titanium is understandable considering its high chemical reactivity, unlike noble metals, such as Au and Ag, that can form pure metal nanoparticles upon ablation in water. The formation of hydrated products has been reported to be favored when using unusual laser focusing configurations, such as when the target is placed below the focus, which causes the breakdown of water [7]. In our study, the laser was focused at the target surface with a f-theta lens within ± 0.01 mm from focus. The absence of other titanium oxides could also be due to phase transformation happening during the laser-induced irradiation of the already-synthesized nanoparticles.

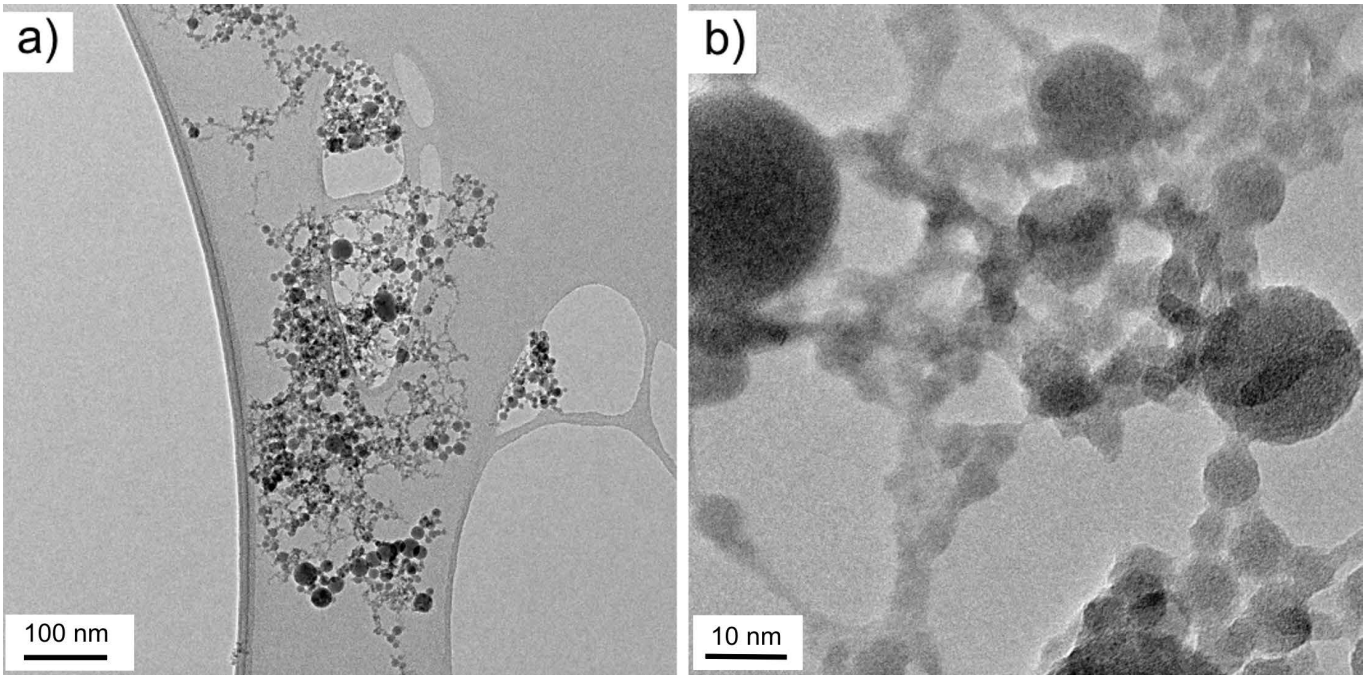

Fig. 2: TEM images show (a) synthesized nanoparticles were spherical with diameters from 3 nm to 32 nm (b) nanoparticles bound in web-like network.

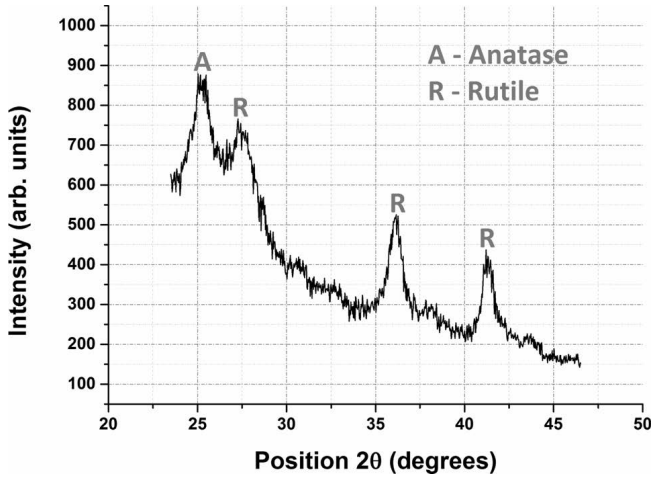

Fig. 3: Wide-angle x-ray scattering pattern shows nanoparticles were rutile and anatase.

The synthesis yield for all the samples was measured according to aforementioned method explained in the experimental section. When plotted against the laser power, the weights of the samples containing nanoparticles followed a trend as shown in Fig. 4. The yield increased from 12 % laser power to 40 % laser power after which it drops at 50 % laser power even though the laser power is increasing.

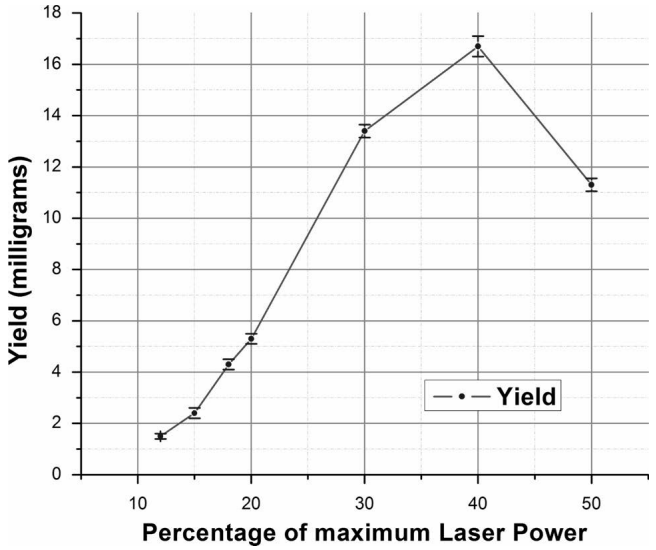

Fig. 4: Graph showing the effect of laser power on synthesis yield of nanoparticles.

To understand this, laser fluence values were determined by measuring spot diameters for the laser beam at different laser powers. Here, laser fluence is defined as the ratio of the laser pulse energy to the laser spot area. The minimum spot diameter was 50 μm and stayed constant till 20 % laser power. However, the spot diameter became larger in value as the laser power was increased from 20 % to finally 100 % of the maximum laser power. Kabashin *et al.* (2003) reported that with the increase in pulse energy, which is synonymous with an increase in laser power, the productivity of nanoparticles increases almost proportionally [14]. Keeping the laser fluence the same, higher spot size leads to increased yield of nanoparticles [10]. In our study, the spot size of the laser remained unchanged with the increase in laser power from 12 – 20 % laser power, and increased from 50 μm at 20 % laser power to only 54.2 μm at 40 % laser power. This led to an almost steady increase in the laser fluence with the increase in laser pulse energy (Fig. 5). Due to this, the productivity of the nanoparticles increased almost linearly with the increase in laser power till 40 % laser power (Fig. 4), which is consistent with results reported by Kabashin *et al.* (2003), mentioned earlier. At 50 % laser power, however, the laser spot size increased with the increase in laser power, resulting in decreased laser fluence. This increase in the spot size has been attributed to the high beam quality factor 3.7 as mentioned in the experimental section earlier. So, the energy of the laser pulse at 50 % laser power was focused on a much larger area compared to 40 % laser power. Due to this, at 50 % laser power, we observed a drop in the yield of nanoparticles. The decrease in the yield is because of two competing laser parameters affecting the ablation rate, namely, increase in pulse energy, and decrease in laser fluence. The ablation rate (units μm/pulse) is the layer thickness of material ablated for a given pulse. The ablation rate increases with increase in pulse energy and laser fluence [13, 14]. At 50 % laser power, compared to 40 % laser power, the competing mechanisms affecting the yield of nanoparticles are (i) reduced ablation rate due to decrease in laser fluence, and (ii) increased ablation due to increased pulse energy leading to higher temperature of plasma causing more ablation by melting and evaporation. However, the increase in laser pulse energy, in this case, was not sufficient to overcome the decrease in laser fluence, and consequently resulted in a decreased yield of nanoparticles. This hypothesis is further supported by comparing the yield at 30 % and 50 % laser power from Fig. 4 in which the yield is higher for 30 % laser power. The laser pulse energy at 30 % and 50 % laser power were 1.02 mJ and 1.70 mJ per pulse respectively. From Fig. 5, the observed laser fluences at 30 % and 50 % laser power were 46.75 J/cm^2 and 41.53 J/cm^2 respectively. The comparison of laser energy and laser fluence at 30 % and 50 % with their corresponding yields indicates that the variation in the yield of nanoparticles follows the variation in the laser fluence. In addition, the variation in the yield of nanoparticles also follows the variation in laser power (and pulse energy) as long as there is insignificant change in the spot diameter, which means a steady increase in laser fluence with the increase in pulse energy. The variation in the spot diameter is a result of high beam quality factor of 3.7. This correlation elucidates the variation of yield with laser power and laser fluence.

The ablation rate increases with higher repetition rate resulting in higher yield because at higher repetition rates up to few tens of kHz, such as 25 kHz in this case, the mean temperature at the laser spot is much higher than room temperature, causing more ablation[10]. At low repetition rates, the time interval between the pulses is long enough for the laser spot to cool down to room temperature. This is however, not possible at high repetition rates such as 25 kHz in our experiments, due to which the mean laser spot temperature is higher. In this study, a 500-ns laser was used, which signifies that the pulse duration was 500 ns. This resulted in overlap of laser pulses with the plasma plume causing plasma shielding of the laser pulses and absorption of energy from laser pulses by the plasma plume.

With a nanosecond laser, the laser pulse and ablated material coexist for longer time as compared to a picosecond or femtosecond laser [10]. This further increases the temperature, pressure and duration of the plasma plume [10]. Due to this, the yield of nanoparticles increases compared to when the laser pulses do not overlap with the plasma plume. This temporal overlapping of subsequent laser pulses on plasma plume improves the homogeneity of the plasma plume, which in turn results in a narrower size distribution compared to ablation with picosecond or femtosecond laser pulses [10]. Furthermore, this increased temperature of the plasma plume also raises the temperature of the target which subsequently increases the yield as the plasma heats up the target to cause more ablation by melting and evaporation [14]. This analysis signifies that long pulse duration (nanosecond laser) and optimum repetition rate of few tens of kHz leads to an increase in the yield of nanoparticles. The yield in TiO_2 nanoparticles from laser ablation of titanium using laser at visible and UV wavelengths is of interest to the authors for future work.

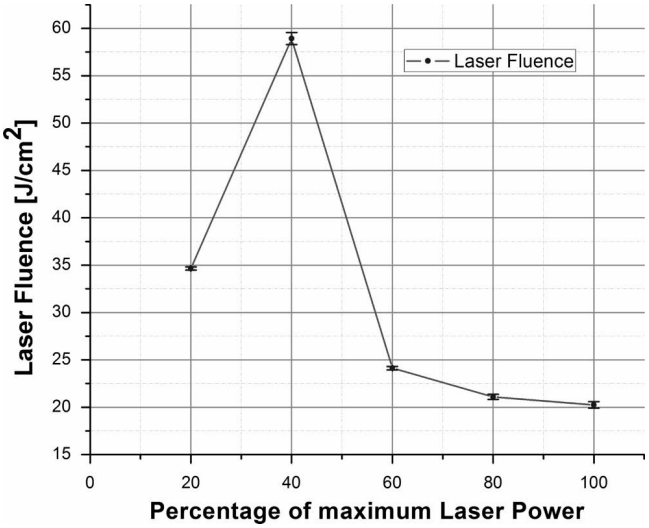

Fig. 5: Graph shows experimentally calculated laser fluence values at different laser powers.

IV. Conclusions

We report the successful synthesis of nanoparticles by PLA of titanium in deionized water at different laser powers and investigated experimentally the variation in the yield of nanoparticles with laser power. TEM results showed spherical nanoparticles 3 – 32 nm in diameter in the nanoparticle suspensions synthesized, forming a web-like network. ED pattern and WAXS results showed that the nanoparticles were crystalline and consisted of two titania allotropes: rutile and anatase. The yield measurements indicated that the synthesis yield of TiO_2 nanoparticles increases linearly with the increase in laser power (synonymous to pulse energy in this study) as long as the laser fluence increases with laser power. When the laser fluence does not increase proportionally with the increase in laser power, then two competing mechanisms determine the synthesis yield: (i) increased ablation rate due to increased pulse energy, and (ii) decreased ablation due to reduction in laser fluence. The analysis showed that the yield increases proportionally with the increase in laser fluence. When the beam quality factor M^2 is high, such as 3.7 in our study, the variation of yield of nanoparticles is described more appropriately by laser fluence than by laser power or pulse energy, since a high M^2 value leads to variation in spot size with the increase in pulse energy. The discussion of the chosen laser parameters revealed that with longer pulse duration and higher repetition rate, the yield of nanoparticles increases.

References

1 Friedmann, D., Mendive, C., Bahnemann, D.: TiO_2 for water treatment: parameters affecting the kinetics and mechanisms of photocatalysis, *Appl. Catal. B Environ.*, **99**, 398 – 406, (2010).

2 Fujishima, A., Rao, T.N., Tryk, D.: Titanium dioxide photocatalysis, *J. Photochem. Photobiol. C Photochem. Rev.,* **1,** 1 – 21, (2000).

3 Machmudah, S., Takada, N., Kanda, H., Sasaki, K., Goto, M.: Fabrication of gold and silver nanoparticles with pulsed laser ablation under pressurized CO_2, *Adv. Nat. Sci. Nanosci. Nanotechnol.,* **4,** 045011, (2013).

4 Saitow, K., Yamamura, T., Minami, T.: Gold nanospheres and nanonecklaces generated by laser ablation in supercritical fluid, *J. Phys. Chem. C,* **112,** 18340 – 18349, (2008).

5 Semaltianos, N. G. *et al.*: Laser ablation in water: A route to synthesize nanoparticles of titanium monoxide, *Chem. Phys. Lett.*, **496,** 113 – 116, (2010).

6 Singh, A. *et al.*: Pulsed laser ablation-induced green synthesis of TiO_2 nanoparticles and application of novel small angle X-ray scattering technique for nanoparticle size and size distribution analysis, *Nanoscale Res. Lett.,* **11,** 447, (2016).

7 Amendola, V., Meneghetti, M.: Laser ablation synthesis in solution and size manipulation of noble metal nanoparticles, *Phys. Chem. Chem. Phys.,* **11,** 3805 – 3821, (2009).

8 Tsuji, T., Okazaki, Y., Tsuboi, Y., Tsuji, M.: Nanosecond time-resolved observations of laser ablation of silver in water, *Jpn. J. Appl. Phys.,* **46,** 1533 – 1535, (2007).

9 Soliman, W., Takada, N., Sasaki, K.: Growth processes of nanoparticles in liquid-phase laser ablation studied by laser-light scattering, *Appl. Phys. Express*, **3**, 035201, (2010).

10 Amendola, V., Meneghetti, M.: What controls the composition and the structure of nanomaterials generated by laser ablation in liquid solution? *Phys. Chem. Chem. Phys.,* **15,** 3027 – 3046, (2013).

11 Altınoğlu, E. İ., Adair, J. H.: Near infrared imaging with nanoparticles. *Wiley Interdiscip. Rev. Nanomedicine Nanobiotechnology*, **2,** 461 – 477. (2010).

12 Yu, D.-Y., Chen, H.-C., Chang, S.-Y., Hsiao, Y.-C., Chang, C.-J.: Comparing the effectiveness of 1064 vs. 810 nm wavelength endovascular laser for chronic venous insufficiency (Varicose Veins), *LASER Ther.,* **22**, 247 – 253, (2013).

13 Vlădoiu, I., Stafe, M., Neguţu, C., Popescu, I. M.: Nanopulsed ablation rate of metals dependence on the laser fluence and wavelength in atmospheric air, *UPB Sci. Bull. Ser. A Appl. Math. Phys.,* **70**, 119 – 126, (2008).

14 Kabashin, A.V., Meunier, M.: Synthesis of colloidal nanoparticles during femtosecond laser ablation of gold in water, *J. Appl. Phys.*, **94**, 7941, (2003).

15 Werner, D., Hashimoto, S.: Improved working model for interpreting the excitation wavelength- and fluence-dependent response in pulsed laser-induced size reduction of aqueous gold nanoparticles, *J. Phys. Chem. C*, **115**, 5063 – 5072, (2011).